Rapid Communications

Phonon- and charged-impurity-assisted indirect free-carrier absorption in Ga_2O_3

Hartwin Peelaers [1,2,*] and Chris G. Van de Walle [2]

[1] *Department of Physics and Astronomy, University of Kansas, Lawrence, Kansas 66045, USA*

[2] *Materials Department, University of California, Santa Barbara, California 93106-5050, USA*

(Received 3 May 2019; revised manuscript received 16 July 2019; published 5 August 2019)

Monoclinic β-Ga_2O_3 has a large band gap of 4.8 eV, and can therefore be used as a contact material that is transparent to visible and UV light. However, indirect free-carrier absorption processes, mediated by either phonons or charged impurities, will set a fundamental limit on transparency. We use first-principles calculations to accurately assess the absorption cross section and to elucidate the microscopic origins of these processes. Phonon-assisted absorption is dominated by the emission of phonons, and is therefore always possible. This indirect absorption is inversely proportional to the cube of the wavelength. The presence of charged impurities, whether intentional or unintentional, leads to additional absorption, but for realistic concentrations, phonon-assisted absorption remains the largest contribution. Direct free-carrier absorption also leads to below-gap absorption, with distinct peaks where optical transitions match energy differences to higher conduction bands. In contrast, indirect absorption uniformly reduces transparency for all sub-band-gap wavelengths.

DOI: 10.1103/PhysRevB.100.081202

Monoclinic β-Ga_2O_3 is being intensively explored for applications based on its an unusual combination of a large band gap (4.76 eV at low temperatures [1,2]) and high *n*-type conductivity. The large band gap leads to high breakdown fields, which are desirable for high-power devices [3,4], and enables applications where transparency in the UV is important, such as transparent contacts for photovoltaics and deep-UV photodetectors [5–7]. The ability to grow large-area single-crystalline substrates [8–10] is also conducive to large-scale adoption of the material.

Even if the pristine material is highly transparent at energies below the band gap, the presence of electrons in the conduction band (which is required for most applications) will lead to sub-band-gap absorption [11]. The material tends to be unintentionally *n* type [12], and controlled doping can readily be achieved [13] using Si [14,15], Sn [16], Ge [17], or even transition metals such as Nb [18,19]. The electrons in the conduction band can absorb photons in two distinct ways: direct transitions to higher-lying conduction bands can occur [11] if they are dipole-allowed; and indirect transitions can be assisted by phonons or ionized impurities. Indirect transitions are weaker than direct transitions, but the momentum provided by the scattering process gives access to a far greater number of final states, thus contributing to the overall strength of this absorption mechanism. Indirect free-carrier absorption is commonly discussed in the infrared by using a phenomenological Drude model, but we will see it can lead to absorption at all wavelengths, which can only be accurately described by more sophisticated modeling.

Here, we use a fully first-principles approach to describe indirect free-carrier absorption in Ga_2O_3 mediated by scattering with phonons or ionized impurities. After describing the computational approach, we present results for phonon-assisted indirect absorption and discuss the different possible final conduction-band states. We address the strength of absorption mediated by phonons versus ionized impurities (where the charged centers can be due to donors as well as compensating defects). Finally we comment on the relative importance of direct versus indirect free-carrier absorption in different wavelength regions. Our results thus reveal the fundamental limits of transparency in doped Ga_2O_3, which is important for future optoelectronic applications, and they allow us to provide insight into recent experimental observations [20,21]. In addition, since optical techniques are frequently employed to characterize the material, detailed knowledge of the mechanisms that can affect transparency at specific wavelengths is essential.

All calculations are performed in the 10-atom primitive cell [22] using density functional theory as implemented in the Quantum ESPRESSO package [23]. We use the local density approximation (LDA) with norm-conserving Troullier-Martin pseudopotentials [24] with an energy cutoff of 70 Ry. The electronic structure was sampled using a $4 \times 4 \times 2$ **k**-point grid. While LDA underestimates the magnitude of the band gap (Fig. 1), its description of the conduction bands is accurate, as compared to hybrid-functional calculations [25], and for indirect free-carrier absorption only the conduction bands are important. We oriented the monoclinic cell so that the **a** axis is parallel to the Cartesian *x* axis, **b** is parallel to *y*, and **c** makes an angle of 13.77° with respect to the *z* axis. Phonons and electron-phonon coupling matrix elements were obtained using density functional perturbation theory [26] on a $32 \times 32 \times 16$ **q**-point grid. The indirect phonon-assisted absorption was computed using Fermi's golden rule,

*peelaers@ku.edu

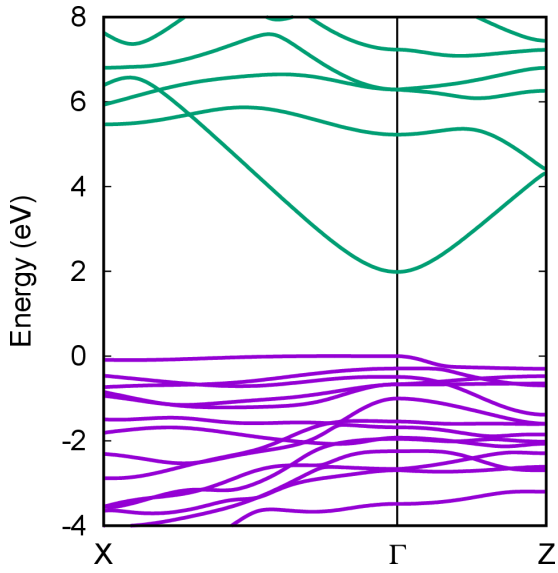

FIG. 1. Band structure along two high-symmetry directions (labeled following Ref. [25]) as calculated with the LDA functional. Valence and conduction bands are indicated with different colors.

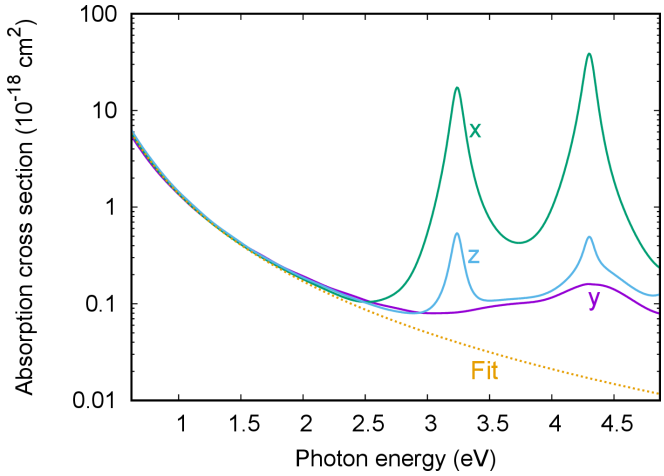

FIG. 2. Absorption cross section for phonon-assisted indirect absorption in Ga_2O_3 as a function of photon energy for light polarized along the three Cartesian directions. The dotted line is a fit to a power law as described in the text.

as outlined in Ref. [27]:

$$\alpha(\omega) = 2\frac{4\pi^2 e^2}{\omega c n_r}\frac{1}{V_{\text{cell}}}\frac{1}{N_{\boldsymbol{k}}N_{\boldsymbol{q}}}\sum_{vijk\boldsymbol{q}}|\hat{\boldsymbol{e}}\cdot(\boldsymbol{S}_1+\boldsymbol{S}_2)|^2 \times\left(n_{v\boldsymbol{q}}+\frac{1}{2}\pm\frac{1}{2}\right)(f_{i\boldsymbol{k}}-f_{j,\boldsymbol{k}+\boldsymbol{q}}) \times\delta(\epsilon_{j,\boldsymbol{k}+\boldsymbol{q}}-\epsilon_{i\boldsymbol{k}}-\hbar\omega\pm\hbar\omega_{v\boldsymbol{q}}). \quad (1)$$

$\hbar\omega$ and $\hat{\boldsymbol{e}}$ are the energy and polarization of the absorbed photon, V_{cell} is the unit-cell volume, n_r the refractive index, $\hbar\omega_{v\boldsymbol{q}}$ the phonon energy, and $\epsilon_{i\boldsymbol{k}}$ the electron energy. $n_{v\boldsymbol{q}}$ is the phonon and $f_{i\boldsymbol{k}}$ the electron occupation number. i and j indicate the band number, v the phonon mode, $\boldsymbol{k}$ and $\boldsymbol{q}$ the wave vectors, and $N_{\boldsymbol{k}}$ and $N_{\boldsymbol{q}}$ are the number of $\boldsymbol{k}$ and $\boldsymbol{q}$ wave vectors. The generalized optical matrix elements $\boldsymbol{S}_1$ and $\boldsymbol{S}_2$ are given by

$$\boldsymbol{S}_1(\boldsymbol{k},\boldsymbol{q}) = \sum_m \frac{\boldsymbol{v}_{im}(\boldsymbol{k})g^{\text{el-ph}}_{mj,v}(\boldsymbol{k},\boldsymbol{q})}{\epsilon_{m\boldsymbol{k}}-\epsilon_{i\boldsymbol{k}}-\hbar\omega+i\eta},$$

$$\boldsymbol{S}_2(\boldsymbol{k},\boldsymbol{q}) = \sum_m \frac{g^{\text{el-ph}}_{im,v}(\boldsymbol{k},\boldsymbol{q})\boldsymbol{v}_{mj}(\boldsymbol{k}+\boldsymbol{q})}{\epsilon_{m,\boldsymbol{k}+\boldsymbol{q}}-\epsilon_{i\boldsymbol{k}}\pm\hbar\omega_{v\boldsymbol{q}}+i\eta}, \quad (2)$$

and correspond to the two possible paths of the indirect absorption process. The upper signs indicate emission of phonons and the lower signs absorption of phonons. $\boldsymbol{v}$ are the dipole matrix elements (calculated using the velocity operator [27]) and g are the electron-phonon coupling matrix elements. The energy-conserving delta function in Eq. (1) was approximated by a Gaussian with width 0.2 eV, which is chosen to obtain converged results for the $32\times32\times16$ **q**-point grid and also smooths out unphysical fluctuations. We added a small imaginary constant ($\eta = 0.05$ eV) to avoid divergences in the denominator of Eqs. (2). This amounts to a Lorentzian broadening. To report results that are independent of the free-carrier concentration, we define the absorption cross section, which is the absorption coefficient α divided by the free-carrier concentration.

For ionized-impurity-assisted absorption we use a screened Coulomb potential and replace the electron-phonon matrix element g in Eq. (2) by

$$g^{\text{impurity}}_{i,j} = \left\langle i,\boldsymbol{k}\left|\frac{4\pi e^2 Z}{\epsilon_0(q^2+q^2_{\text{scr}})}\right|j,\boldsymbol{k}+\boldsymbol{q}\right\rangle, \quad (3)$$

where Z is the charge, and q_{scr} is the screening wave vector, modeled using Thomas-Fermi screening, as we consider degenerate doping situations [28]. In this model we do not take into account explicit atomic relaxations around the defect. Implicitly, some of these effects are included through the static dielectric constant ϵ_0, which includes the screening by ions and electrons.

Due to the low symmetry of monoclinic β-Ga_2O_3 (symmetry group $C2/m$), optical absorption is anisotropic. We therefore consider absorption of light polarized along the three Cartesian directions. We focus on indirect absorption below the band gap; at higher energies, across-the-gap absorption is dominant. In Fig. 2 we show the results for indirect phonon-assisted absorption. For photon energies below 2.5 eV, the indirect absorption is close to isotropic. This is because it arises purely from intraband absorption in the lowest conduction band, and this band has low anisotropy [11,29]. Similar isotropic free-carrier absorption has been observed experimentally [21]. The decrease in absorption with increasing photon energy can be modeled with a power-law dependence on the photon energy, as shown by the dotted line in Fig. 2, which is a fit to a power law for photon energies between 0.6 and 1.5 eV for light polarized along x. The fitted exponent is -3.01 for the x direction, -2.92 for y, and -3.06 for z. Results for other transparent conducting oxides, such as SnO_2 and In_2O_3 [27,30,31], also indicate that the exponent is -3. A simple Drude expression, assuming the free-carrier scattering time is independent of frequency, would yield an exponent of -2 [32]. If the conduction band is approximated to have a linear dispersion relation (which is a good approximation

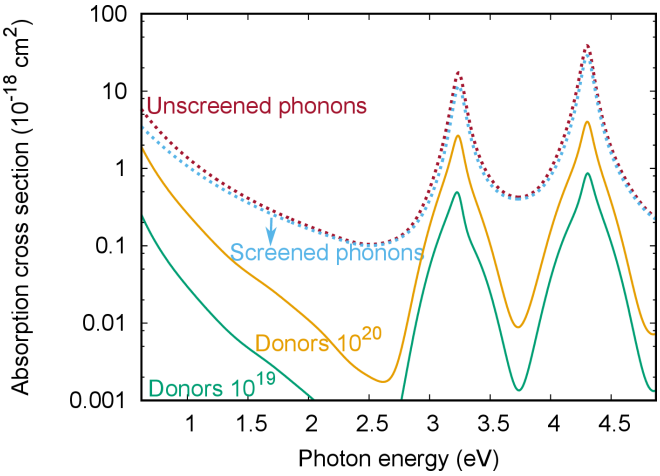

FIG. 3. Absorption cross section for light polarized along x due to charged-impurity-assisted scattering, for two different donor concentrations (10^{19} and 10^{20} cm^{-3}). For reference, the phonon-assisted scattering is depicted with a dotted line, for unscreened phonons (also shown in Fig. 2), and for phonons screened by 10^{19} cm^{-3} free carriers.

for Ga_2O_3 [11,29]) one can derive that the exponent should be -3 [30]. We also analyzed experimental absorption data obtained for different free-carrier concentrations [20,21]. If we add a constant, photon-energy independent absorption, the data also fits a -3 power law, indicating that for these samples phonon-assisted indirect absorption is (besides the constant absorption) the dominant absorption process. The presence of this constant background absorption, combined with systematic higher absorption coefficients reported experimentally, indicates that the fundamental absorption limits are not yet reached in experimental samples.

For photon energies above 2.5 eV, an increase in optical absorption is observed, and strong anisotropy is evident. Absorption for light polarized along x (and to a lesser extent light polarized along z) shows two strong absorption peaks, centered around 3.24 and 4.30 eV. We note that the precise shape and magnitude of these absorption peaks depend sensitively on the choice of η in Eq. (2) (the Lorentzian broadening). The appearance of these peaks is related to the fact that strong vertical transitions can take place from the lowest CB to higher-lying CBs (see Fig. 1). Ultimately, such transitions are better described by calculating direct optical absorption (as we did in Ref. [11], where peaks indeed appear at these same energies). Such absorption has recently been observed as well [21].

Near a surface or interface, some concentration of free carriers can be achieved in a thin layer through gating or modulation doping. In general, however, the presence of free carriers in the bulk of a material requires introducing donor impurities. Once ionized, these dopants can lead to scattering processes that provide momentum for indirect absorption processes, similar to scattering by electron-phonon interactions.

In Fig. 3 we compare indirect absorption assisted by phonons and by ionized impurities. Since the phonon-assisted absorption shown before in Fig. 2 did not consider the effect of screening by the free carriers, we will include this screening by replacing the calculated electron-phonon matrix elements g by $g(\boldsymbol{k},\boldsymbol{q})q^2/(q^2+q_{\rm scr}^2)$, where $q_{\rm scr}$ is the Thomas-Fermi screening length, calculated using ϵ_∞ [33]. We first compare the absorption due to unscreened phonons and due to phonons screened by 10^{19} cm^{-3} free carriers (dotted lines). The largest effect is seen for smaller photon energies, corresponding to transitions assisted by long-wavelength (small q) phonons, and including screening leads to a reduction of the absorption.

Next we consider two ionized donor impurity concentrations: 10^{19} and 10^{20} cm^{-3}, the latter corresponding to the highest reported carrier concentration [17]. The results in Fig. 3 show that phonon-assisted absorption is always stronger, even at the high dopant concentration. Compensation of donors can occur, and Ga vacancies are the most likely compensating centers [34,35]. These vacancies occur in a $3-$ charge state and hence act as much stronger scattering centers: the matrix elements [Eq. (3)] are proportional to the defect charge Z, and enter squared in Eq. (1). Absorption assisted by Ga vacancies will therefore be nine times stronger than for the same concentration of singly charged defects. The total observed absorption will be the sum of phonon-assisted and charged-impurity-assisted scattering, the latter being due to both donor impurities and any compensating defects.

Given that 10^{20} cm^{-3} is the highest reported carrier concentration [17], our results show that even at this density phonon-assisted scattering is stronger than impurity-assisted scattering. However, if the samples are compensated, the total concentration of charged impurities and defects in the sample could be much larger than the carrier concentration, and impurity-assisted scattering could then become a limiting factor. Compensation should therefore be avoided.

We also note the different wavelength dependence of the phonon-assisted (proportional to the cube of the wavelength) and charged-impurity-assisted absorption. This can be explained by the different q dependence of the associated matrix elements: for longitudinal optical phonon modes this is proportional to $1/q$ (as in the Fröhlich model [36]), while for impurities this is proportional to $1/q^2$ [see Eq. (3), when ignoring the screening wave vector $q_{\rm scr}$]. Our analysis of the experimental data presented in Refs. [20,21] showed that for these samples, with free-carrier concentrations up to 10^{19} cm^{-3}, phonon-assisted absorption is the dominant absorption process, as the best power-law fit yielded an exponent of -3.

Based on our calculations, we can estimate what the consequences of phonon-assisted indirect free-carrier absorption are for visible-light absorption in a typical substrate. Since this absorption process is unavoidable, this will form the fundamental limit on the transparency. We will assume red visible light (1.7 eV) polarized along the x direction and a carrier concentration of 10^{17} cm^{-3}, a typical background doping density. The calculated absorption coefficient is 0.03 cm^{-1} (see Fig. 3). For a 300-μm-thick sample, the transmission would then be $\exp(-\alpha d) = 0.999$, so very good transparency. For a highly doped thin film, assuming a carrier concentration of 10^{20} cm^{-3} (highest reported doping density [17]), that would mean an absorption coefficient of 28.6 cm^{-1}. For a 1-μm-thick sample, the transmission would then be 0.997; still very good transparency in a highly doped thin film.

In conclusion, we have presented fully first-principles calculations of the phonon- and charged-impurity-assisted indirect absorption in monoclinic Ga_2O_3. These indirect absorption processes lead to intraband transitions and sub-band-gap absorption inversely proportional to the cube of the photon energy (or proportional to the cube of the photon wavelength). Sub-band-gap transitions to higher conduction bands are also possible, but in this case a description as direct transitions is more appropriate. Additional indirect absorption is due to scattering from charged donors, but also from compensating defects, such as Ga vacancies. Nevertheless, for realistic donor and compensating defect concentrations, the phonon-assisted absorption remains the main indirect absorption process. Based on our comparison with available experimental data, current samples are not yet displaying the transparency consistent with the fundamental limits on absorption.

This work was supported by the GAME MURI of the Air Force Office of Scientific Research (FA9550-18-1-0479). Computing resources were provided by the Center for Scientific Computing supported by the California NanoSystems Institute and the Materials Research Science and Engineering Center (MRSEC) at UC Santa Barbara through NSF DMR 1720256 and NSF CNS 1725797, and by the Extreme Science and Engineering Discovery Environment (XSEDE), which is supported by NSF Grant No. ACI-1548562.

[1] H. H. Tippins, Phys. Rev. **140**, A316 (1965).
[2] T. Matsumoto, M. Aoki, A. Kinoshita, and T. Aono, Jpn. J. Appl. Phys. **13**, 737 (1974).
[3] M. Higashiwaki, K. Sasaki, H. Murakami, Y. Kumagai, A. Koukitu, A. Kuramata, T. Masui, and S. Yamakoshi, Semicond. Sci. Technol. **31**, 034001 (2016).
[4] S. J. Pearton, J. Yang, P. H. Cary, F. Ren, J. Kim, M. J. Tadjer, and M. A. Mastro, Appl. Phys. Rev. **5**, 011301 (2018).
[5] A. K. Chandiran, N. Tetreault, R. Humphry-Baker, F. Kessler, E. Baranoff, C. Yi, M. K. Nazeeruddin, and M. Grätzel, Nano Lett. **12**, 3941 (2012).
[6] T. Minami, Y. Nishi, and T. Miyata, Appl. Phys. Express **6**, 044101 (2013).
[7] T. Oshima, T. Okuno, and S. Fujita, Jpn. J. Appl. Phys. **46**, 7217 (2007).
[8] N. Ueda, H. Hosono, R. Waseda, and H. Kawazoe, Appl. Phys. Lett. **70**, 3561 (1997).
[9] H. Aida, K. Nishiguchi, H. Takeda, N. Aota, K. Sunakawa, and Y. Yaguchi, Jpn. J. Appl. Phys. **47**, 8506 (2008).
[10] Z. Galazka, R. Uecker, K. Irmscher, M. Albrecht, D. Klimm, M. Pietsch, M. Brützam, R. Bertram, S. Ganschow, and R. Fornari, Cryst. Res. Technol. **45**, 1229 (2010).
[11] H. Peelaers and C. G. Van de Walle, Appl. Phys. Lett. **111**, 182104 (2017).
[12] M. Lorenz, J. Woods, and R. Gambino, J. Phys. Chem. Solids **28**, 403 (1967).
[13] J. B. Varley, J. R. Weber, A. Janotti, and C. G. Van de Walle, Appl. Phys. Lett. **97**, 142106 (2010).
[14] E. G. Víllora, K. Shimamura, Y. Yoshikawa, T. Ujiie, and K. Aoki, Appl. Phys. Lett. **92**, 202120 (2008).
[15] K. Sasaki, M. Higashiwaki, A. Kuramata, T. Masui, and S. Yamakoshi, Appl. Phys. Express **6**, 086502 (2013).
[16] D. Gogova, M. Schmidbauer, and A. Kwasniewski, CrystEngComm **17**, 6744 (2015).
[17] E. Ahmadi, O. S. Koksaldi, S. W. Kaun, Y. Oshima, D. B. Short, U. K. Mishra, and J. S. Speck, Appl. Phys. Express **10**, 041102 (2017).
[18] W. Zhou, C. Xia, Q. Sai, and H. Zhang, Appl. Phys. Lett. **111**, 242103 (2017).
[19] H. Peelaers and C. G. Van de Walle, Phys. Rev. B **94**, 195203 (2016).
[20] Z. Galazka, K. Irmscher, R. Uecker, R. Bertram, M. Pietsch, A. Kwasniewski, M. Naumann, T. Schulz, R. Schewski, D. Klimm, and M. Bickermann, J. Cryst. Growth **404**, 184 (2014).
[21] O. Koksal, N. Tanen, D. Jena, H. G. Xing, and F. Rana, Appl. Phys. Lett. **113**, 252102 (2018).
[22] H. Peelaers, D. Steiauf, J. B. Varley, A. Janotti, and C. G. Van de Walle, Phys. Rev. B **92**, 085206 (2015).
[23] P. Giannozzi, S. Baroni, N. Bonini, M. Calandra, R. Car, C. Cavazzoni, D. Ceresoli, G. L. Chiarotti, M. Cococcioni, I. Dabo, A. Dal Corso, S. de Gironcoli, S. Fabris, G. Fratesi, R. Gebauer, U. Gerstmann, C. Gougoussis, A. Kokalj, M. Lazzeri, L. Martin-Samos, N. Marzari, F. Mauri, R. Mazzarello, S. Paolini, A. Pasquarello, L. Paulatto, C. Sbraccia, S. Scandolo, G. Sclauzero, A. P. Seitsonen, A. Smogunov, P. Umari, and R. M. Wentzcovitch, J. Phys.: Condens. Matter **21**, 395502 (2009).
[24] N. Troullier and J. L. Martins, Phys. Rev. B **43**, 1993 (1991).
[25] H. Peelaers and C. G. Van de Walle, Phys. Status Solidi B **252**, 828 (2015).
[26] S. Baroni, S. de Gironcoli, A. Dal Corso, and P. Giannozzi, Rev. Mod. Phys. **73**, 515 (2001).
[27] H. Peelaers, E. Kioupakis, and C. G. Van de Walle, Phys. Rev. B **92**, 235201 (2015).
[28] N. W. Ashcroft and N. D. Mermin, *Solid State Physics* (Holt, Rinehart and Winston, New York, 1976).
[29] Y. Kang, K. Krishnaswamy, H. Peelaers, and C. G. Van de Walle, J. Phys.: Condens. Matter **29**, 234001 (2017).
[30] H. Peelaers, E. Kioupakis, and C. G. Van de Walle, Appl. Phys. Lett. **100**, 011914 (2012).
[31] H. Peelaers, E. Kioupakis, and C. G. Van de Walle, arXiv:1907.13573 (2019).
[32] H. Y. Fan, Rep. Prog. Phys. **19**, 107 (1956).
[33] B. Ridley, *Quantum Processes in Semiconductors* (Clarendon, Oxford, 1982).
[34] J. B. Varley, H. Peelaers, A. Janotti, and C. G. Van de Walle, J. Phys.: Condens. Matter **23**, 334212 (2011).
[35] E. Korhonen, F. Tuomisto, D. Gogova, G. Wagner, M. Baldini, Z. Galazka, R. Schewski, and M. Albrecht, Appl. Phys. Lett. **106**, 242103 (2015).
[36] H. Fröhlich, Adv. Phys. **3**, 325 (1954).